Hindawi Publishing Corporation
Advances in Meteorology
Volume 2014, Article ID 791256, 20 pages
http://dx.doi.org/10.1155/2014/791256

Research Article

Wind Velocity Decreasing Effects of Windbreak Fence for Snowfall Measurement

Ki-Pyo You and Young-Moon Kim

Department of Architecture Engineering, Chonbuk National University, 567 Baekje-daero, deokjin-gu, Jeonju-si, Jeollabuk-do 561-756, Republic of Korea

Correspondence should be addressed to Ki-Pyo You; youkp@jbnu.ac.kr

Received 26 September 2013; Revised 23 January 2014; Accepted 23 January 2014; Published 16 March 2014

Academic Editor: Sven-Erik Gryning

Meteorological observatories use measuring boards on even ground in open areas to measure the amount of snowfall. In order to measure the amount of snowfall, areas unaffected by wind should be found. This study tried to determine the internal wind flow inside a windbreak fence, identifying an area unaffected by wind in order to measure the snowfall. We performed a computational fluid dynamics analysis and wind tunnel test, conducted field measurements of the type and height of the windbreak fence, and analyzed the wind flow inside the fence. The results showed that a double windbreak fence was better than a single windbreak fence for decreasing wind velocity. The double fence (width 4 m, height 60 cm, and fixed on the bottom) has the greatest wind velocity decrease rate at the central part of octagonal windbreak.

1. Introduction

Fresh snowfall is defined as new snow covering an even plane. The depth of snowfall is defined as the increment of the snow layer cover during the time of measurement. The snow depth is generally measured each day and the snowfall is reported in centimeters per day. The depth of fresh snowfall on open ground can be measured directly using scaled rulers or a snow ruler. The depth of snow covering the ground, or accumulated onthe ground, is measured by inserting a scaled rod vertically into the ground. However, snow covering the ground may come into the measurement plate by wind. Another limitation is that the snow ruler might meet an ice layer, rather than the ground. Thus, it is difficult to obtain a representative height measurement in an open area. We need to make sure that the total depth, including the ice layer, is measured and we need to average multiple measurements from each observation. The amount of snowfall measured in open areas is greatly affected by wind. Piles of snow formed by frequently blowing wind are scattered, resulting in some difficulty in evaluating the exact amount of snowfall. Current studies have focused on diverse equipment to measure the exact amount of snowfall. In addition, snowfall equipment is installed in areas where snowfall is not particularly influenced by wind. However, there is no research on wind control at the point where the amount of snowfall is measured. There has been much research undertaken on windbreak fences. In 1971, Plate [1] subdivided diverse air current areas in relation to turbulence boundary layers near windbreak fences. Based on the results of research into wind decrease areas at the back sides of fences, a diversity of windbreak fences has been used. Perera [2] and Ranga Raju et al. [3] reported that the wake phenomenon disappeared on the back side of the fence when a windbreak fence with a porosity of 30% was installed. Judd et al. [4] tested wind tunnels on the flow around single and multiple porous windbreaks sheltering a model plant canopy. They found that a windbreak has effects on the flow within the sheltered canopy, both upwind and downwind of the break. There is an acceleration within the canopy just upwind of the break, in contrast with a deceleration above the canopy. Lee and Kim [5] and Park and Lee [6] performed a wind pressure experiment in a triangular open air storage yard, changing the height of the windbreak fence, porosity, and interval, and reported that their best results were achieved with a porosity of 30–40%. Research on windbreak fences has focused on changes in porosity rates that are aimed at

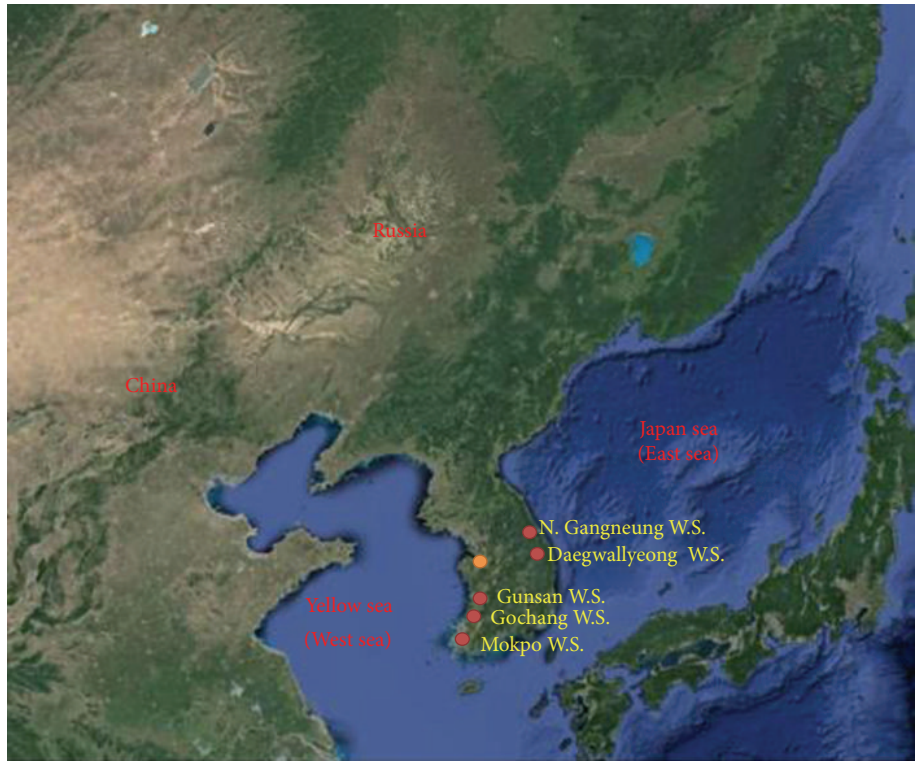

Figure 1: Location of weather station.

decreasing the wind velocity and turbulence caused by back streams within the fences. However, research on windbreak fences and their use in measuring snowfall aims to decrease wind velocity and minimize the effects by wind when snow is piled. In order to achieve this goal, an evaluation was made using three methods. A decrease in wind velocity is considerably affected by a windbreak fence's height and width. In light of this, a computational fluid dynamics (CFD) analysis was conducted in order to determine its optimal form. A wind tunnel test was conducted in order to examine actual wind velocity and its turbulence-decreasing effect at the windbreak fence, using the CFD analysis results. Field measurements for analysis and verification of experimental results were made.

2. Data and Methodology

In order to determine the height of a windbreak fence and experimental wind velocity, the amount of snowfall and wind velocity was analyzed using data on weather conditions over five recent years (2008–2012). Data from weather stations located in western and eastern coastal areas (where heavy snowfalls occur) was the primary source. In the western coastal area, data from weather stations in Gochang (35°20′N, 126°35′E), Gunsan (36°00′N, 126°76′E), and Mokpo (34°81′N, 126°38′E) were used, while in the eastern coastal area, weather stations in northern Gangneung (37°80′N, 128°85′E) and Daegwallyeong (37°67′N, 128°71′E) were analyzed. Figure 1 shows the locations of the weather stations. Figure 2 shows the frequency of snowfall and the frequency of wind velocity over five recent years. In the western coastal area of the peninsula, snow falls more frequently than it does in the east, due to high atmospheric pressure from Siberia and the water temperature of the western region. Nevertheless, a large amount of snow falls in the east coastal area due to high atmospheric pressure from Siberia and the water temperature and mountain ranges. The average amount of snowfall in three areas, with a high frequency of snowfall in the west coast, was 3.6 cm, while the maximum amount of snowfall was measured at 24.5 cm at Gochang weather station, which is located inland. In 90% of the surveyed areas, the frequency of snowfall was less than 10 cm. In more than 50% of the surveyed areas, the frequency of snowfall was less than 2 cm. On the east coast, the average amount of snowfall in two areas where snow fell frequently was 8.75 cm and the largest amount of snow fell in northern Gangneung, which is located inland, at 77.7 cm. The areas where snowfall frequency was less than 10 cm accounted for 75% of the total frequency. The areas where the frequency of snowfall was smaller than 5 cm made up more than 57% of the total frequency. Regarding wind velocity distribution during snowfall, the average wind velocity of three areas in the west coast was 3 m/s and the maximum wind velocity was 11.2 m/s, at the Mokpo weather station. During snowfall, the frequency of wind velocity at less than 6 m/s amounted to 82% of the total frequency. The average wind velocity of two areas on the east coast was 2.5 m/s, with the maximum wind velocity, measured at Daegwallyeong weather station, being 12.4 m/s. During snowfall, the frequency of wind velocity at less than 6 m/s amounted to 96% of the total frequency. Using data from weather stations, the height of windbreaks for snowfall

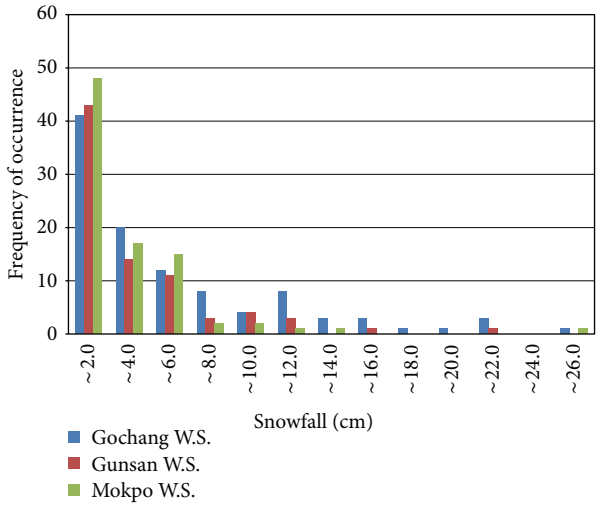

(a) Snowfall frequency of occurrence of the western coastal area

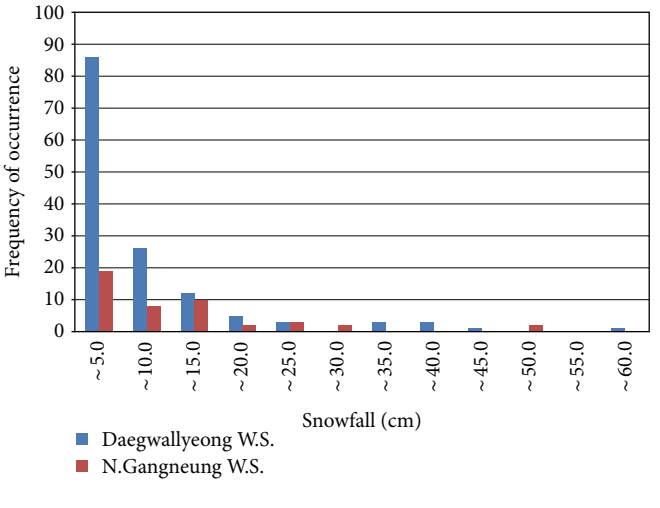

(b) Snowfall frequency of occurrence of the eastern coastal area

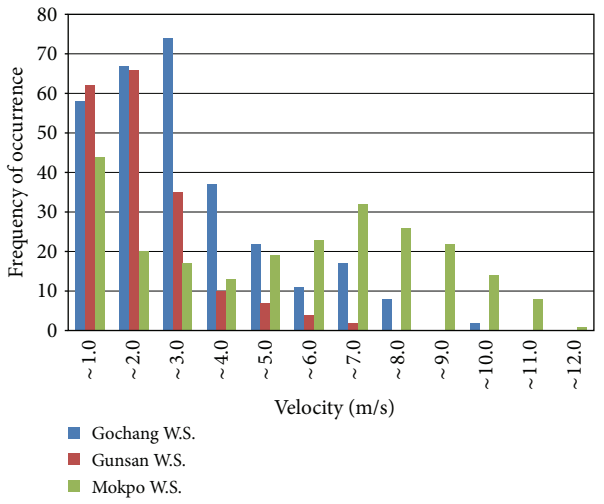

(c) Wind velocity frequency of occurrence of the western coastal area

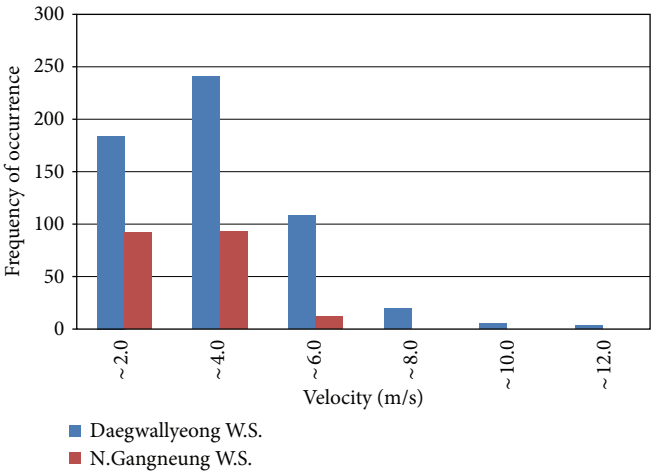

(d) Wind velocity frequency of occurrence of the eastern coastal area

Figure 2: Snowfall frequency of occurrence and wind velocity frequency of occurrence.

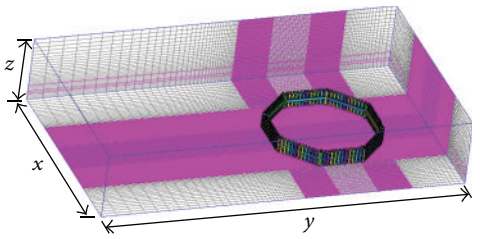

Figure 3: The analyzed domains of CFD.

measurement was determined to range from 40 cm to 80 cm, and the experimental wind velocity was determined to be between 3 m/s and 6 m/s.

3. Computer Fluid Dynamics

3.1. Geometric Model and Mathematical Model. The geometric model of the windbreak fences exhibits suburban conditions. The dimensions of the linear windbreaks and the windbreak fences according to the analysis model were 5 m(x) × 20 m(y) × 4 m(z) and 10 m(x) × 14 m(y) × 4 m(z), respectively, with the parallelepiped situated at the center. Figure 3 shows the analyzed domains. As the meshes for the analyzed domains, 0.5 mm triangular meshes were used. The number of meshes of the analyzed domains was between 1,100,000 and 1,500,000. Commercial software scStream V9.0 was used for the CFD simulation [7]. As a representative model that can simulate flow around the fences, the standard k-ε model was used. The standard k-ε model has excellent convergence properties and is mathematically simple. Its calculation time is also short. Several studies have used CFDs to model wind flow around buildings by solving mass and momentum conservation equations:

$$\frac{\partial \rho}{\partial t} + \nabla \cdot (\rho \vec{v}) = 0,$$
$$\frac{\partial \rho}{\partial t}(\rho \vec{v}) + \nabla \cdot (\rho \vec{v} \vec{v}) = -\nabla p + \nabla \cdot \left(\bar{\bar{\tau}}\right) \rho \vec{g}. \quad (1)$$

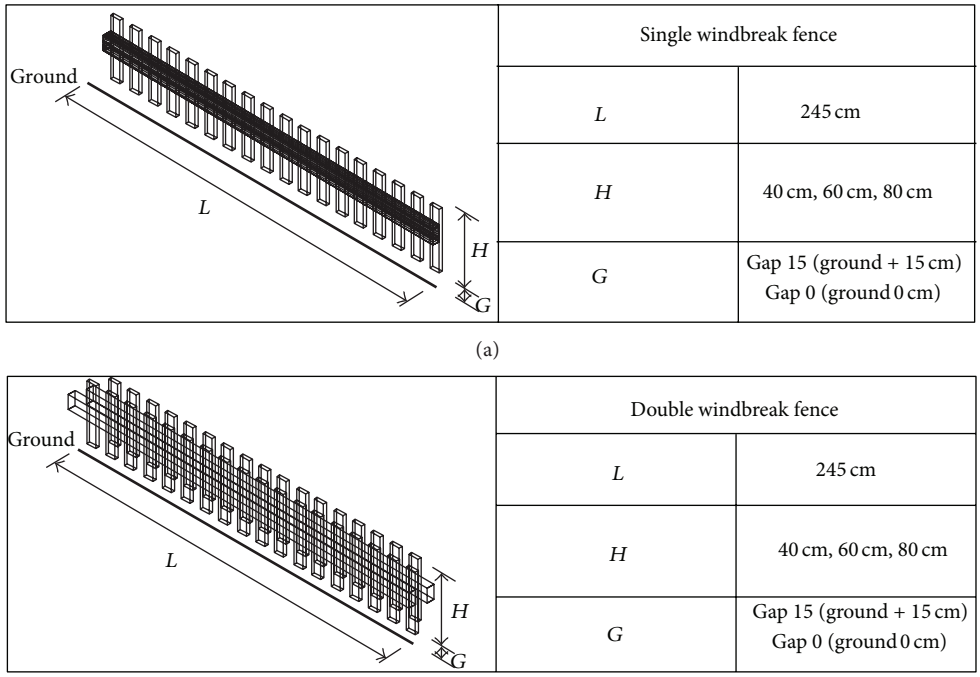

Figure 4: Dimension of the CFD Model for linear windbreak fences.

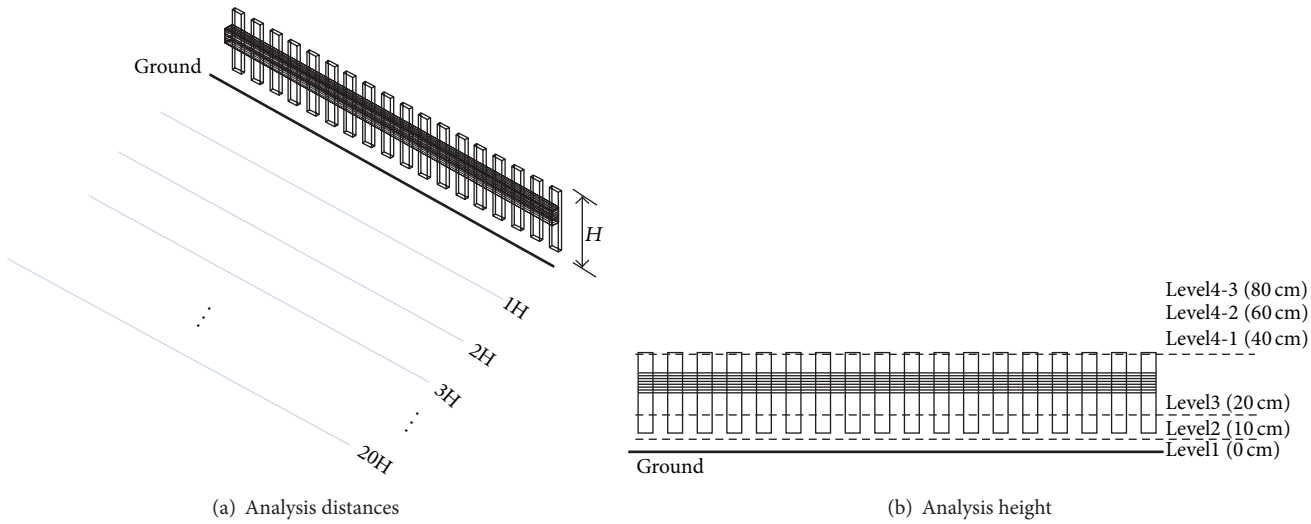

Figure 5: Analysis distances (1H–20H) and heights (LEVEL1–LEVEL4) of the linear windbreak fences.

Here, ρ is the density, p is the static pressure, $\vec{v}$ is the velocity tensor, and $\overline{\overline{\tau}}$ is the stress tensor.

The turbulence kinetic energy, k, is obtained from the following equation [8, 9]:

$$\frac{\partial}{\partial t}(\rho k) + \frac{\partial}{\partial x_i}(\rho k u_i) = \frac{\partial}{\partial x_j}\left[\left(\mu + \frac{\mu_t}{\sigma_k}\right)\frac{\partial k}{\partial x_j}\right] + P_k + P_b - \rho\varepsilon - Y_M + S_k, \quad (2)$$

whereas rate of dissipation ε can be obtained from the equation below:

$$\frac{\partial}{\partial t}(\rho\varepsilon) + \frac{\partial}{\partial x_i}(\rho k u_i) = \frac{\partial}{\partial x_j}\left[\left(\mu + \frac{\mu_t}{\sigma_k}\right)\frac{\partial k}{\partial x_j}\right] + C_{1\varepsilon}\frac{\varepsilon}{k}(P_k + C_{3\varepsilon}P_b) - C_{2\varepsilon}\rho\frac{\varepsilon}{k} + S_\varepsilon. \quad (3)$$

The term in the above equation, P_k, represents the generation of turbulence kinetic energy due to the mean velocity gradients. P_b is the generation of turbulence kinetic energy

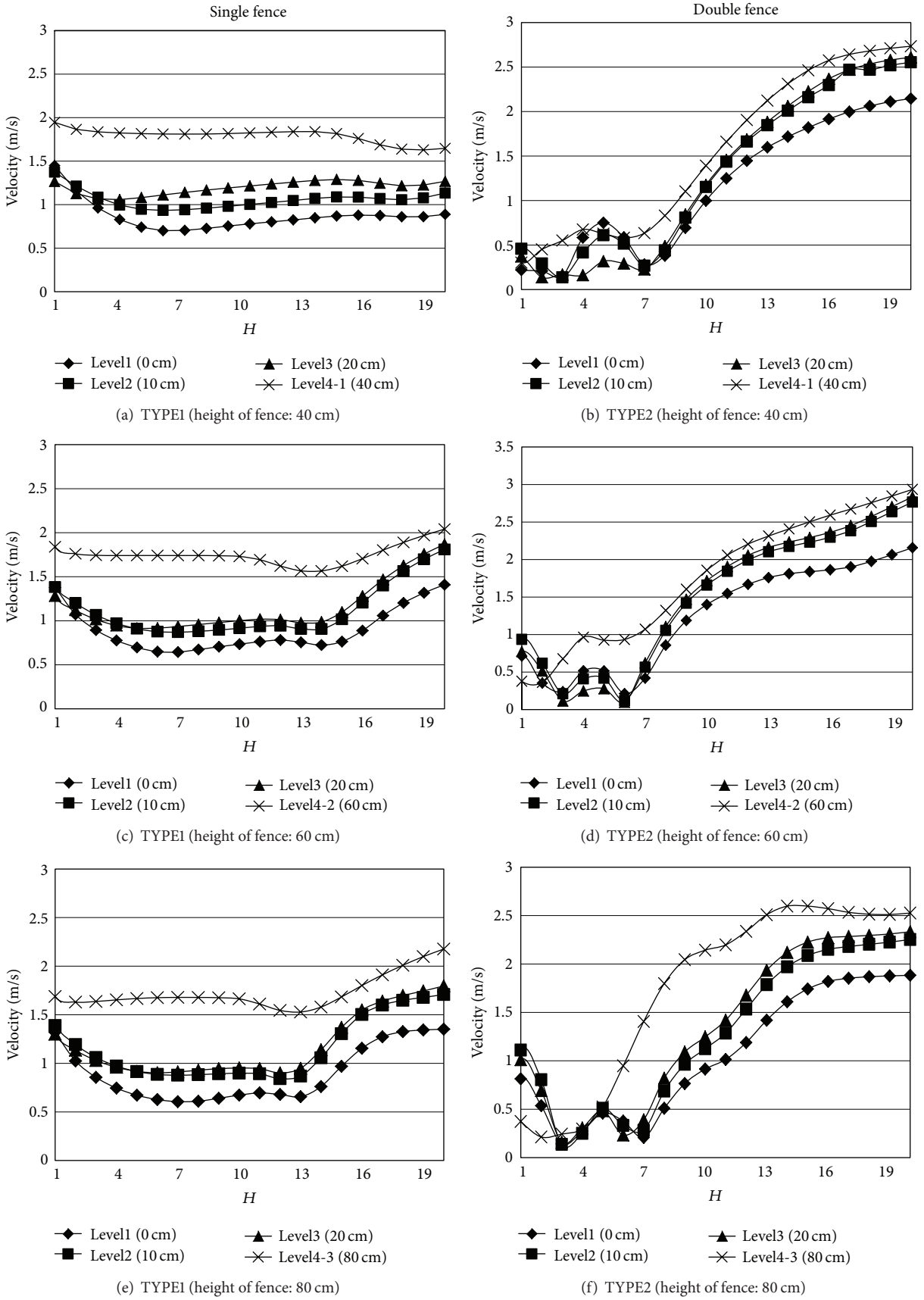

(a) TYPE1 (height of fence: 40 cm)

(b) TYPE2 (height of fence: 40 cm)

(c) TYPE1 (height of fence: 60 cm)

(d) TYPE2 (height of fence: 60 cm)

(e) TYPE1 (height of fence: 80 cm)

(f) TYPE2 (height of fence: 80 cm)

Figure 6: Wind velocity distribution of the linear windbreak fence by distance (GAP 0 cm, reference velocity = 3 m/s).

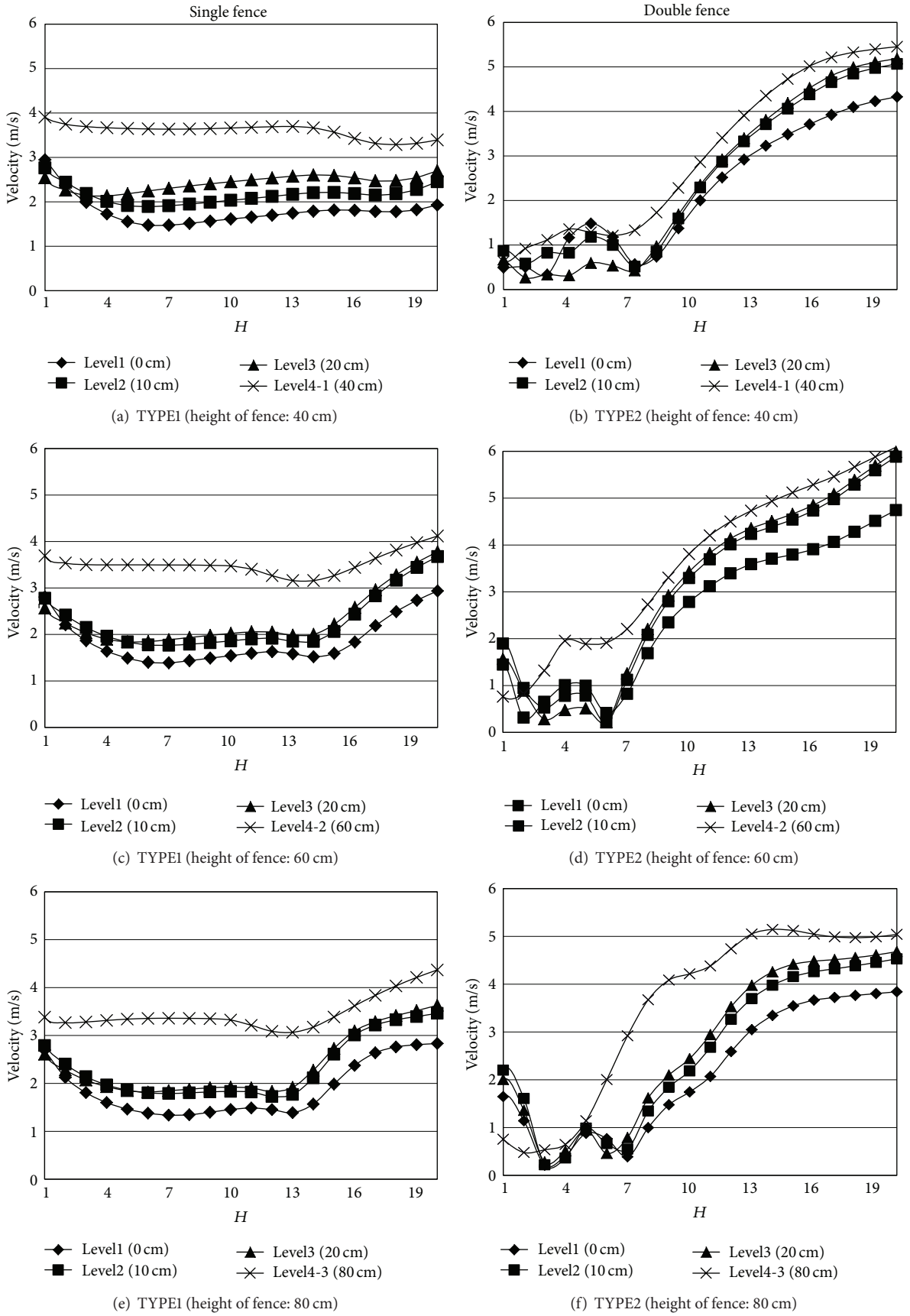

(a) TYPE1 (height of fence: 40 cm)

(b) TYPE2 (height of fence: 40 cm)

(c) TYPE1 (height of fence: 60 cm)

(d) TYPE2 (height of fence: 60 cm)

(e) TYPE1 (height of fence: 80 cm)

(f) TYPE2 (height of fence: 80 cm)

Figure 7: Wind velocity distribution of the linear windbreak fence by distance (Gap 0 cm, reference velocity = 6 m/s).

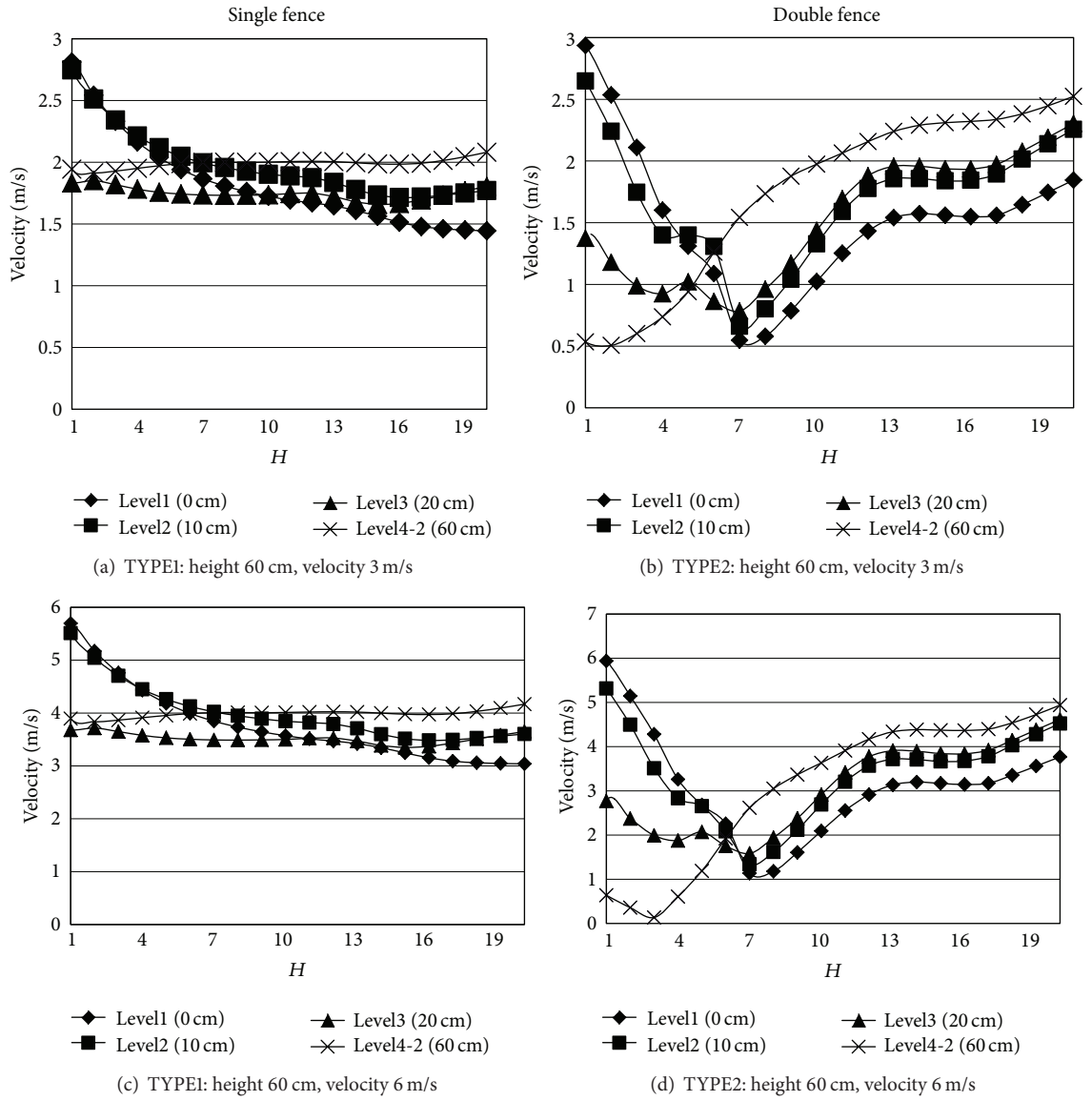

Figure 8: Wind velocity distribution of the linear windbreak fence by distance (Gap 15 cm, reference velocity = 3 m/s, 6 m/s).

due to buoyancy, while Y_M represents the contribution of the fluctuating dilatation in compressible turbulence to the overall dissipation rate. The model constants $C_{1\varepsilon}$, $C_{2\varepsilon}$, C_μ, σ_k, and σ_ε have been determined by Laundar and Saplding [10]:

$$C_{1\varepsilon} = 1.44, \qquad C_{2\varepsilon} = 1.92, \tag{4}$$

$$C_\mu = 0.09, \qquad \sigma_k = 1.0, \qquad \sigma_\varepsilon = 1.3. \tag{5}$$

3.2. Linear Windbreak Fences. Figure 4 shows the dimensions of the CFD model for the linear windbreak fences analysis. Figure 5 shows the analysis distances (1H–20H) and heights (LEVEL1–LEVEL4) of the linear windbreak fences. The analysis range, aimed at examining wind velocity distribution in the back side of the fences, varies according to the height of the fences. Analysis was made up to 800 cm (20H), with the fence height at 40 cm and up to 1,600 cm (20H), with the fence height at 80 cm. The analysis heights of Level1, Level2, and Level3 were set at 0 cm, 10 cm, and 20 cm, regardless of the fence height. Analysis of Level4 was made at 40 cm (Level4-1), 60 cm (Level4-2), and 80 cm (Level4-3), according to the height of the fences. Two types of linear windbreak fence were tested: single (TYPE1) and double (TYPE2). Two heights of fence installation were tested: one with no gap and one with a 15 cm gap from the ground. To assess the linear windbreak fence effects with different wind velocities, we tested wind velocities of 3 m/s and 6 m/s.

3.2.1. Simulation Results. This study has analyzed the downwind and vertical velocity distributions scaled by the height of the fence (H). It has interpreted the distance-based wind

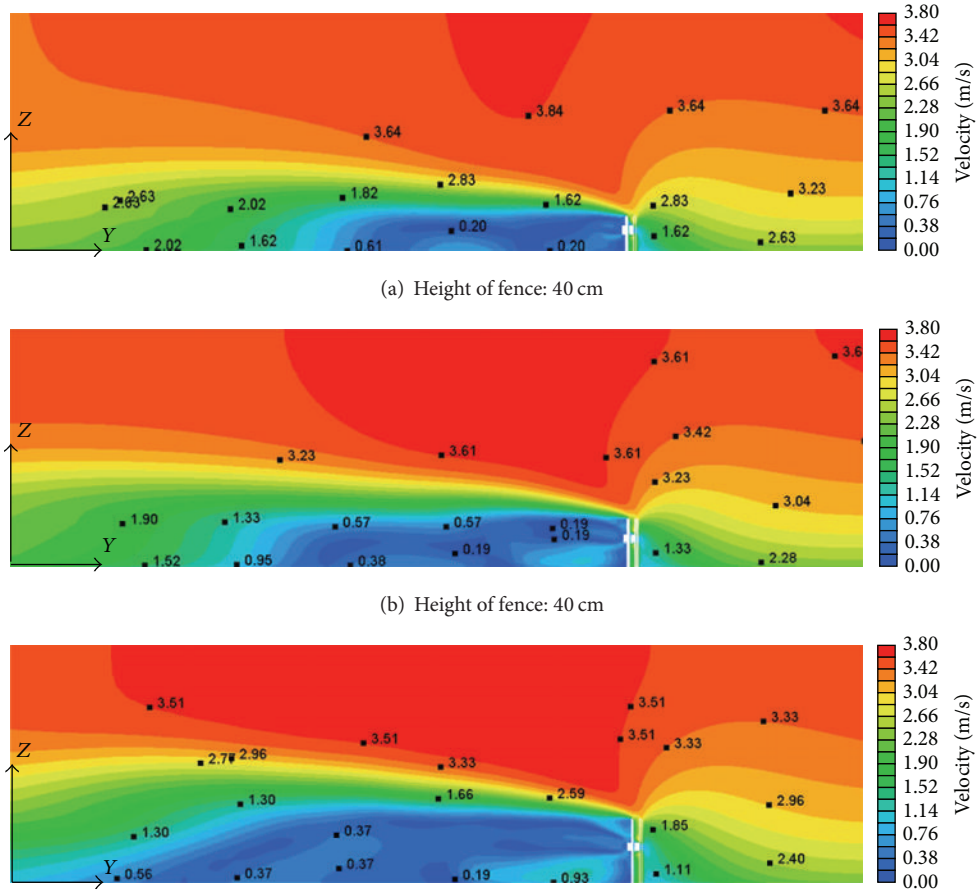

(a) Height of fence: 40 cm

(b) Height of fence: 40 cm

(c) Height of fence: 80 cm

Figure 9: Wind velocity flow the double windbreak fence by height (velocity 3 m/s).

velocity distribution up to the range of 1H–20H. The vertical wind velocity distribution on the downwind side of the fences has been interpreted at the central point of the fence. Figures 6 and 7 show the wind velocity of linear windbreak fences that the distance is normalized with the height of the fence (H). The decrease in wind velocity on the downwind sides of the single fences and double fences (with the windbreak fence's vertical bars fixed on the ground) is influenced by the distance from the fences and the fence height. Regardless of fence height, the wind velocity was regularly decreased to the power of 1H–7H. However, it was influenced by fence height when the distance was more than 7H. With a fence height of 40 cm, the wind velocity was almost regularly distributed up to 7H–20H on the downwind sides of the fences. However, with a fence height of 60 cm, the wind velocity was regularly distributed only up to 7H–15H and increased at heights higher than 15H. With a fence height of 80 cm, the wind velocity was regularly distributed only up to 7H–13H and increased at the heights higher than 13H. Unlike the single fences, the double fences showed great changes in wind velocity distant from their downwind sides. The wind velocity at the 1H point of the double fences decreased in comparison with the same point of the single fences by a maximum of 80% or more. Moreover, the wind velocity at the positions of 3H and 6H, distant from the downwind side of the fence, rapidly decreased to 0.1 m/s regardless of experimental wind velocity. The wind velocity increased regardless of fence height at positions more distant than 6H. These phenomena, different from those with single fences, are believed to occur due to the thickness of the fences increasing by double. The wind velocity distribution at the vertical heights of 0–20 cm (Level1-Level3) of the double fences was almost identical up to 1H–3H. However, within the range of 3H–7H, the wind velocity varied with fence heights. While the wind velocity was the lowest at the 20 cm (Level3) point of the vertical height of the fences, it remained constant at the 80 cm point (Level4-3), regardless of vertical fence heights. Figure 8 shows the analysis at the fence with a 60 cm (Level4-2) height, in order to identify the effects of the gap between the vertical bars of the windbreak fence and the ground. In the case of the single fences, the fastest wind velocity was measured at the point of 1H, distant from the downwind side of the fences at the vertical heights of 0 cm (Level1) and 10 cm (Level2), but the wind velocity decreased until the distance reached the 7H

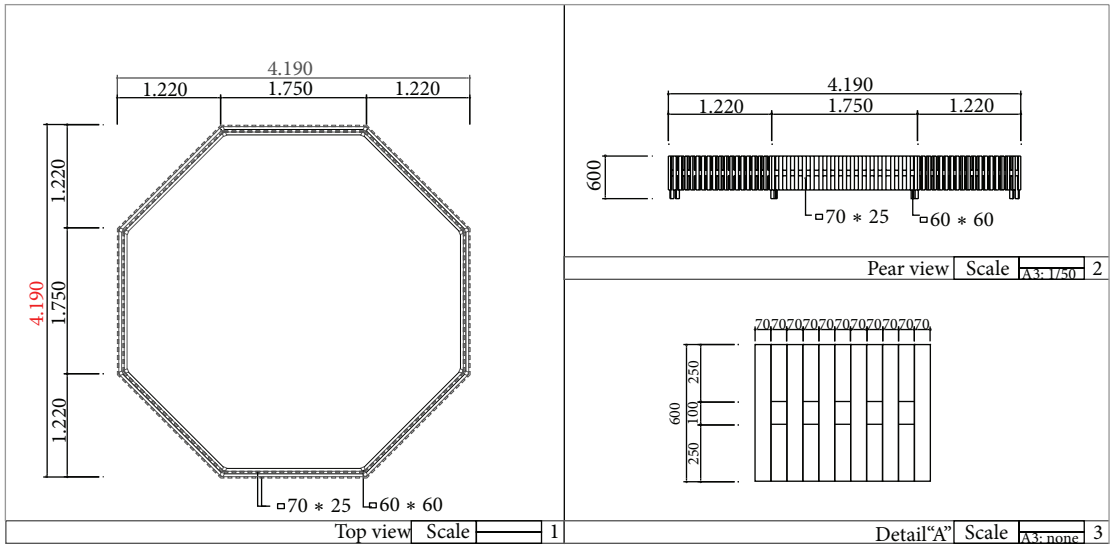

(a) CASE 1 (width: 4 m)

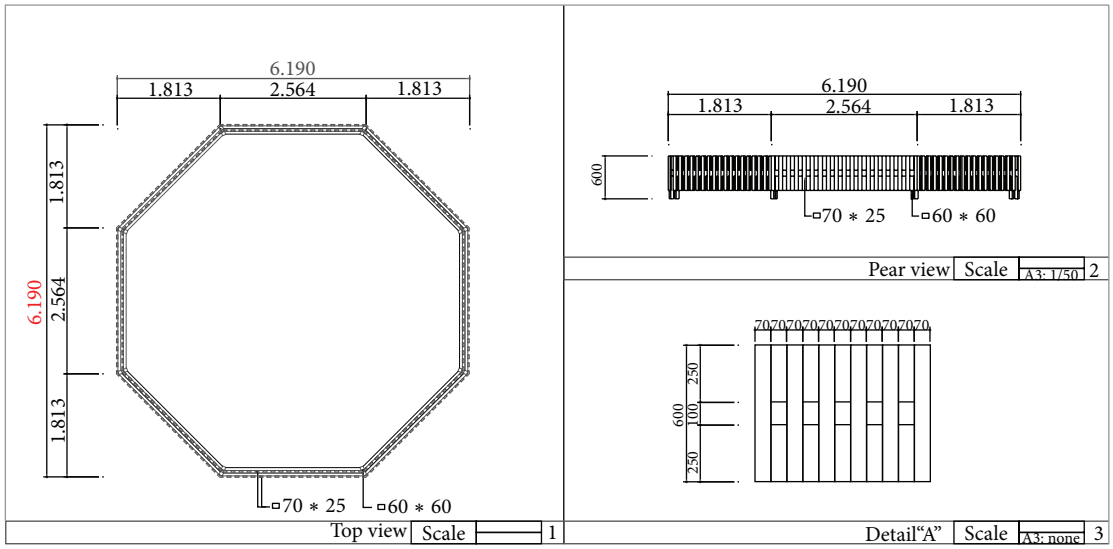

(b) CASE 2 (width: 6 m)

Figure 10: Specifications of the octagonal windbreak fence.

point, after which the wind velocity was almost identically maintained. The wind velocity at the vertical heights of 20 cm (Level3) and 60 cm (Level4-2) was almost regularly distributed at every distance for interpretation, but the wind velocity distribution was 35% slower at 1H–7H, with vertical heights of 0 cm (Level1) and 10 cm (Level2). This was because of gaps in the vertical windbreak fence bars, at a height of 15 cm from the ground. In distance-based changes in wind velocity, the effects of a decrease in wind velocity were less than in the cases of the windbreak fence's vertical bars set on the ground. In the case of the double fences, like the case of the single fences, the wind velocity decreased at the points of 0 cm (Level1) and 10 cm (Level1), when the distance was within the range from 1H to 7H, and then increased when the distance was more than 7H. The wind velocity decreased by 83% or more at the distance of 7H than at 1H. However, with fence heights of 20 cm (Level3) and 60 cm (Level4-2), the wind velocity continuously increased after the greatest amount decreased around 1H. Figure 9 shows wind velocity flow inside of the double windbreak fences by height. The reference wind velocity was 3 m/s, and the wind velocity flow on the downwind side showed up diversely, according to fence heights. The effects of reduced wind velocity on the downwind side of the fences can be identified in a wide area. It was identified that wind velocity greatly decreased, as flow separated from the upper part of the fence within a certain distance range was reattached on the bottom. Wind velocity decrease rates were great around 8H, at a fence height of 40 cm, and around 2H–4H at a fence height between 60 cm and 80 cm.

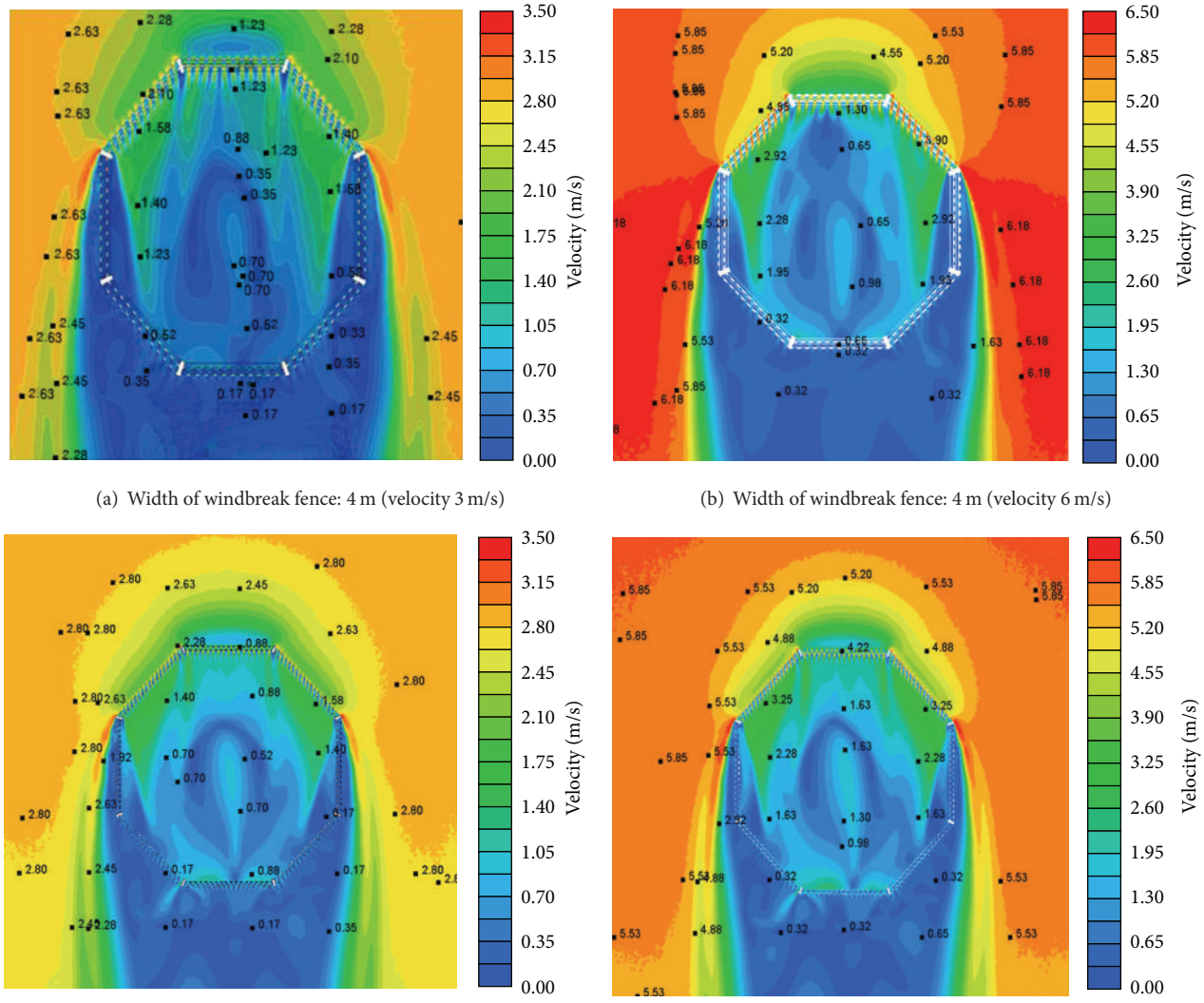

(a) Width of windbreak fence: 4 m (velocity 3 m/s)

(b) Width of windbreak fence: 4 m (velocity 6 m/s)

(c) Width of windbreak fence: 6 m (velocity 3 m/s)

(d) Width of windbreak fence: 6 m (velocity 6 m/s)

Figure 11: Internal wind velocity flow at a measurement height of 10 cm according to the windbreak fence width.

3.3. Octagonal Windbreak Fence. Based on a wind flow analysis of the linear windbreak fence, we found a double fence with a 6 m length that was fixed to the ground to be the most effective. The wind direction will vary in a natural environment, so we analyzed the internal wind flow characteristics by installing an octagonal type windbreak, while considering the direction of the wind. After the octagonal windbreak fence was installed, we determined the width of the fence. Two fence widths (4 m and 6 m) were tested, based on the simulation of the linear fence. Figure 10 shows a CAD (Computer Aided Design) drawing of the fence. The baseline wind velocities were 3 m/s and 6 m/s at fence height. The wind direction was from the front.

3.3.1. Simulation Results. Figures 11 and 12 show the wind velocity flow inside and outside the fence, at heights of 10 cm and 20 cm, depending on the width of the octagonal windbreak fence. The internal wind flow appeared to be constant, regardless of the width. There were large wind velocity decrease effects at the left and right edges of the vertical windbreak fence and in the center of the fence. The wind velocity decrease in the center of the fence had a "U" shape. The 6 m fence had a more obvious "U"-shaped wind decrease than the 4 m fence. The wind flow distribution was not significantly different as the wind velocity increased. The magnitude of the wind velocity decrease in the center of the fence's inside was larger with the 4 m fence than it was with the 6 m fence. The wind flow outside the windbreak fence was almost the same, so it appeared that the external wind flow was not affected by the width of the fence. Figure 13 shows the wind velocity flow inside the fence by height. When the fence was detached from the ground by 15 cm, the wind entering below the bottom of the fence affected the wind velocity at the depth on the opposite side of the fence and affected the internal wind flow. However, when the windbreak fence's

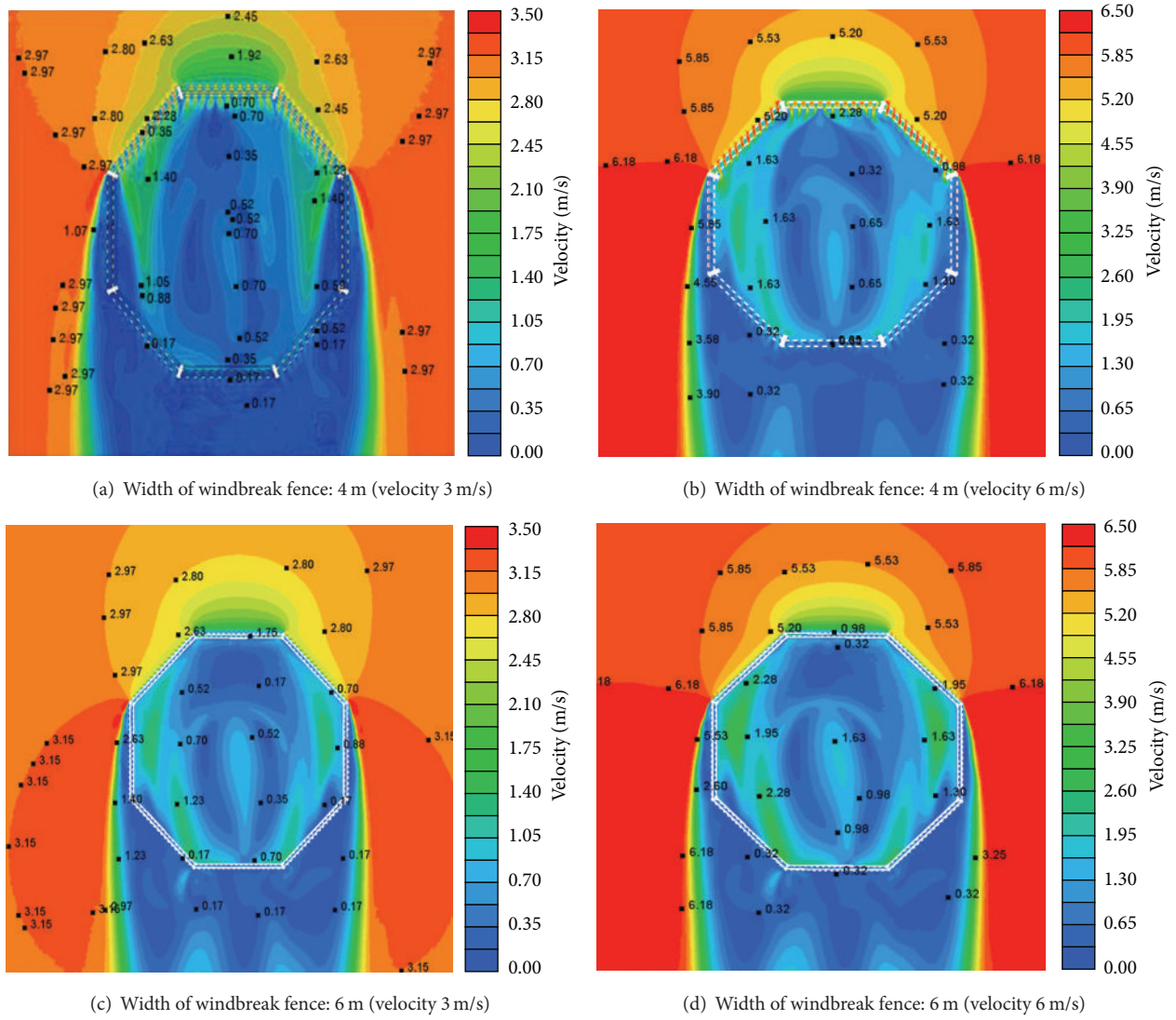

(a) Width of windbreak fence: 4 m (velocity 3 m/s)

(b) Width of windbreak fence: 4 m (velocity 6 m/s)

(c) Width of windbreak fence: 6 m (velocity 3 m/s)

(d) Width of windbreak fence: 6 m (velocity 6 m/s)

FIGURE 12: Internal wind velocity flow at a measurement height of 20 cm according to the windbreak fence width.

vertical bars were attached to the ground, the wind only affected up to a certain distance and it had no major effects on the internal wind flow. The vortex shedding, separated from the top of the upwind side of the fence, had effects on the opposite side. The vortex created at the upwind of the 4 m fence crossed to the opposite side of the fence but did not cross to the opposite side of the 6 m fence. Instead, it remained inside the fence and affected the internal wind flow.

4. Wind Tunnel Test

A wind tunnel test was performed to analyze the wind flow inside the windbreak fence. Wind tunnel tests were conducted in an open-type wind tunnel located at the Department of Architectural Engineering, Chonbuk National University, which has a test section of 1.5 m (width) × 1.7 m (height) and 20 m (length). The boundary layer flow condition, representing natural wind flow over suburban terrain, indicated that the power law exponent of the mean longitudinal wind velocity profile was 0.15 and that the longitudinal turbulence intensity was about 16% at the top of the building model. Terrain category C, as described in the Standard Design Loads for Building, 2010, Architectural Institute of Korea, was simulated over the test section using spires and wooden blocks [11, 12]. The vertical distribution of the mean longitudinal wind velocities and the longitudinal turbulence intensities is shown in Figure 14. The wind tunnel test model was made of balsa wood. Table 1 shows the full-scale size of the experimental model and the model size. Two windbreak fence widths (6 m and 4 m) were used in the experiment. The windbreak fence was attached to the ground and the scale of the model was 1/5. The baseline wind velocity was assumed to be 3 m/s or 6 m/s at the height of the windbreak fence. Because the model was reduced, the wind velocity had

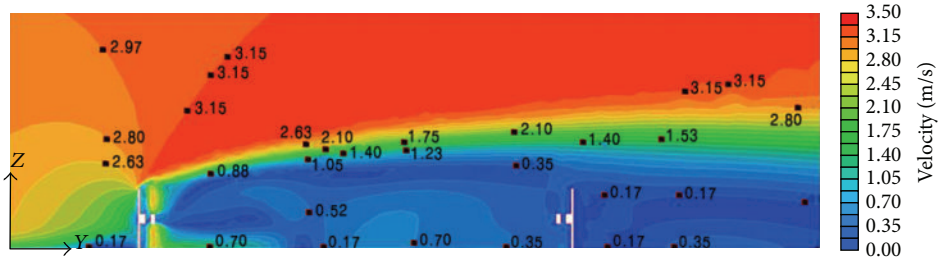

(a) Width of windbreak fence: 4 m, velocity: 3 m/s

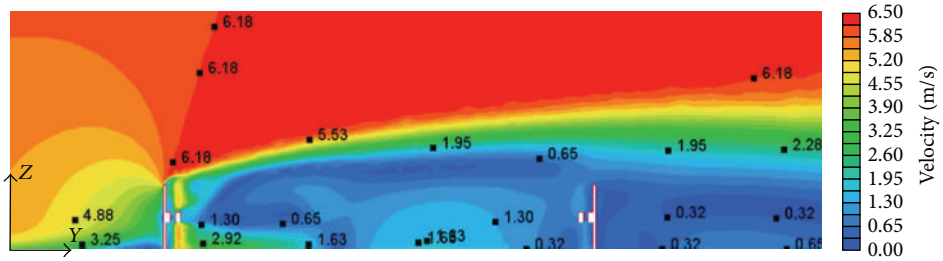

(b) Width of windbreak fence: 4 m, velocity: 6 m/s

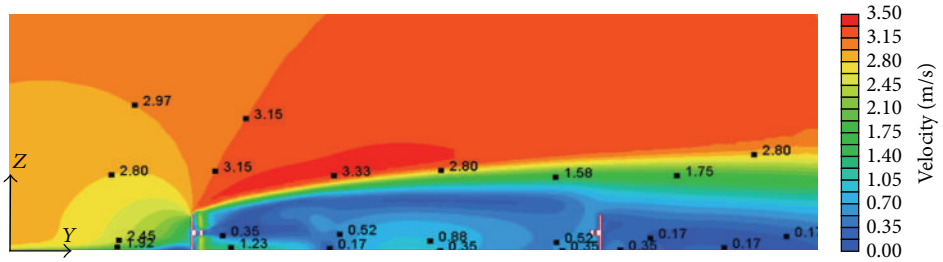

(c) Width of windbreak fence: 6 m, velocity: 3 m/s

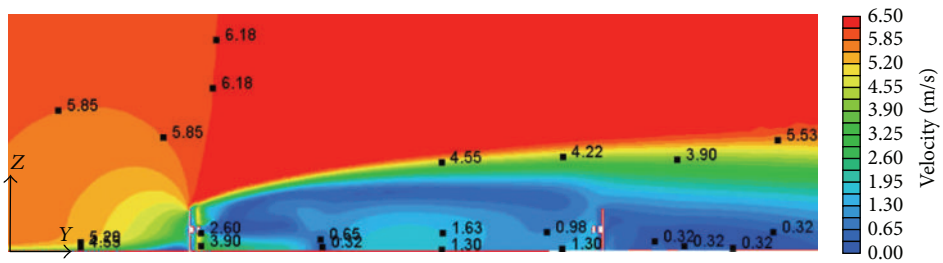

(d) Width of windbreak fence: 6 m, velocity: 6 m/s

Figure 13: Wind velocity flow inside the fence by height.

to be decreased accordingly, which was calculated using (6). The scale of the wind velocity was calculated as the square root of the geometrical scale of the model. We used 1.34 m/s and 2.68 m/s as the experimental wind velocities. The heights inside the fence model were 2 cm and 4 cm, which were equivalent to full-scale sizes of 10 cm and 20 cm. Figures 15 and 16 show the wind velocity measurement locations for the windbreak fences, measuring 0.8 m wide (full-scale size: 4 m, CASE 1) and 1.2 m wide (full-scale size: 6 m, CASE 2), respectively. We measured 25 points for CASE 1 and 45 points for CASE 2. The width of the fence was constant because it was an octagonal, but the internal wind flow of the 6 m width was measured using a rectangular shape. The full-scale wind flow inside the fence was analyzed by measuring (horizontally and vertically) inside the fence at regular intervals:

$$\frac{V_{\text{model}}}{V_{\text{full}}} = \sqrt{\frac{B_{\text{Model}}}{B_{\text{full}}}}. \tag{6}$$

The average wind velocity and turbulence intensity changed according to the location analyzed. The nondimensional average velocity used in the experimental analysis was calculated using (7), while the nondimensional turbulence intensity was calculated using

$$\frac{V}{V_0}, \tag{7}$$

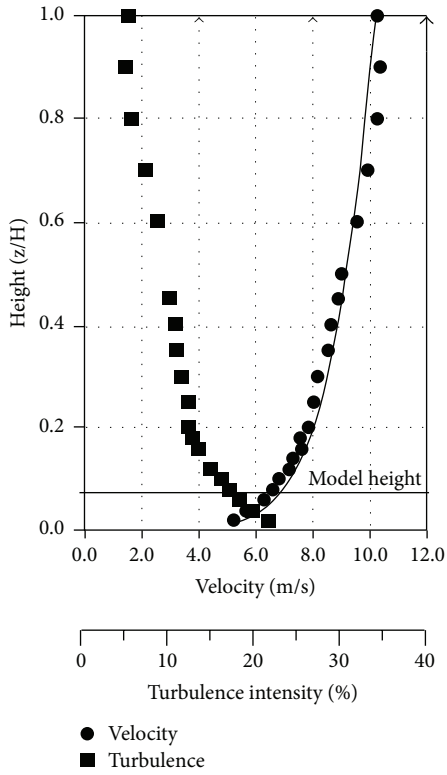

Figure 14: Vertical distribution of the mean longitudinal wind velocities and turbulence intensities.

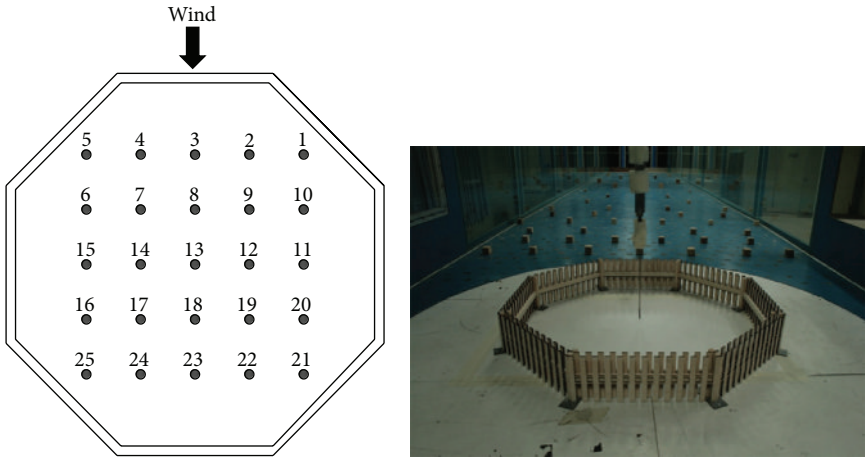

(a) Velocity measurement location (b) Model

Figure 15: Wind velocity measurement locations and CASE 1 model installed in the wind tunnel.

where V: average wind velocity in the measurement location and V_0: wind velocity at the height of the fence

$$\frac{I}{I_0}, \tag{8}$$

where I: turbulence intensity in the measurement location and I_0: turbulence intensity at the height of the fence.

Figures 17 and 18 show the distribution of wind velocity change rates within the windbreaks, whose widths are 4 m and 6 m. In the case of the fences with a width of 4 m, the wind velocity decrease rate was greatest at the center of the fences. When the measured height was 2 cm, the wind velocity decrease rate was greater in the downwind part of the fences, where wind blows, than in the upwind part. When the measured height was 4 cm, the rates of wind velocity

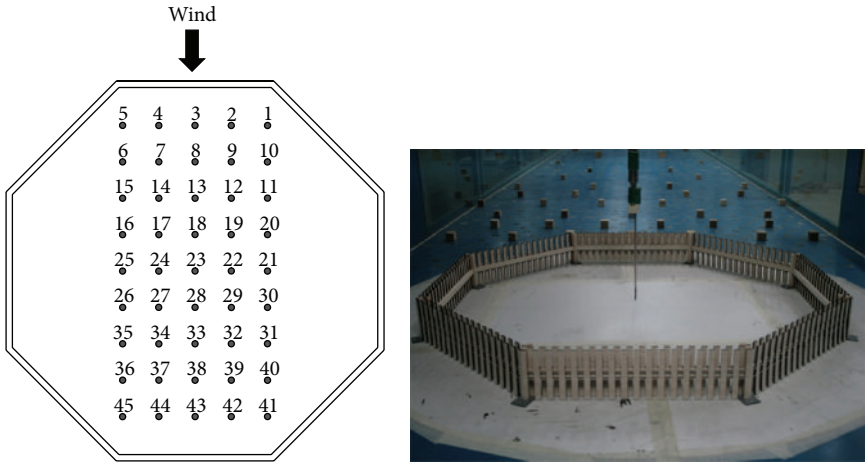

(a) Velocity measurement location (b) Model

Figure 16: Wind velocity measurement locations and CASE 2 model installed in the wind tunnel.

Table 1: Specifications of the windbreak fence used in the wind tunnel test (unit = m).

	Width		Height	
	Full-scale	Model	Full-scale	Model
Case A	4	0.8	0.6	0.12
Case B	6	1.2	0.6	0.12

decreases in the downwind and upwind parts of the fences were the same. This is thought to be due to the fact that the wind separated at the upwind parts of the fences hit the downwind parts of the fences and then flew downward. Even though the reference wind velocity increased, the wind velocity decrease rates at the center of the fences were the same, at 78%. The wind velocity decrease rate for the internal wind flow was the same, according to the wind velocity increase with the measurement height. With the width of 6 m, the wind flow was measured in the shape of a rectangle and the wind flow was represented as a rectangular shape. In contrast to the width of 4 m, the wind velocity decrease rate was the highest at the upwind part of the width of 6 m from where the wind blew. The wind flow characteristics, according to the height and baseline wind velocity, were the same as those with the width of 4 m. However, the increased fence width increased the wind velocity at the back of the fence. Figures 19 and 20 show the distribution of the turbulence intensity inside the windbreak fence, according to the fence width. The turbulence intensity inside the windbreak fence was lowest at the upwind part and at the edge of the fence. Above 0.5 H, there was a constant turbulence intensity distribution. As the wind velocity increased, the turbulence intensity became smaller and it was constant, regardless of the height. This confirms that the turbulence was constant inside the windbreak fence. The width of 6 m (CASE 2) had a lower turbulence intensity than the width of 4 m (CASE 1).

5. Comparative Analysis of the CFD and Wind Tunnel Tests

We compared the wind tunnel test results and the CFD results. The CFD simulation was performed using the same size of model and the same wind velocity as the wind tunnel test. The CFD simulation and wind tunnel test results were compared with CASE 1 (fence width 4 m). We used 1.38 m/s and 2.68 m/s as the wind velocities in the wind tunnel test. The wind velocity distribution heights inside the windbreak fence were 2 cm and 4 cm. Figure 21 shows the wind velocity distribution and the correlation coefficients for the wind tunnel test and CFD, according to the wind velocity. The correlation coefficients of the CFD and wind tunnel tests were distributed in a range of 0.7-0.8, regardless of wind velocity and measurement height. The correlation coefficient was close to 1, which confirmed that there was a strong correlation between the wind tunnel test and the CFD results.

6. Field Measurements

The windbreak fences for field measurement included two fences, one with a width of 6 m and one with a width of 4 m. The height of the windbreak fences was constant at 60 cm. The windbreak's vertical bars were fixed on the bottom. Table 2 shows the components of the models used for field measurement. The measuring instrument used for field measurement consisted of four three-cup anemometers (JY-WS161C) and two data loggers (JDL-74A) to automatically store measured data. A total of four anemometers were installed, one within each of the three windbreak models and one outside the windbreak models, between models A and C. The anemometers installed at the center inside the windbreak fences had a height of 20 cm. Figure 22 shows the arrangement plan and measurement process of anemometers. The anemometers had received a performance test by the Korea Meteorological Industry Promotion Agency

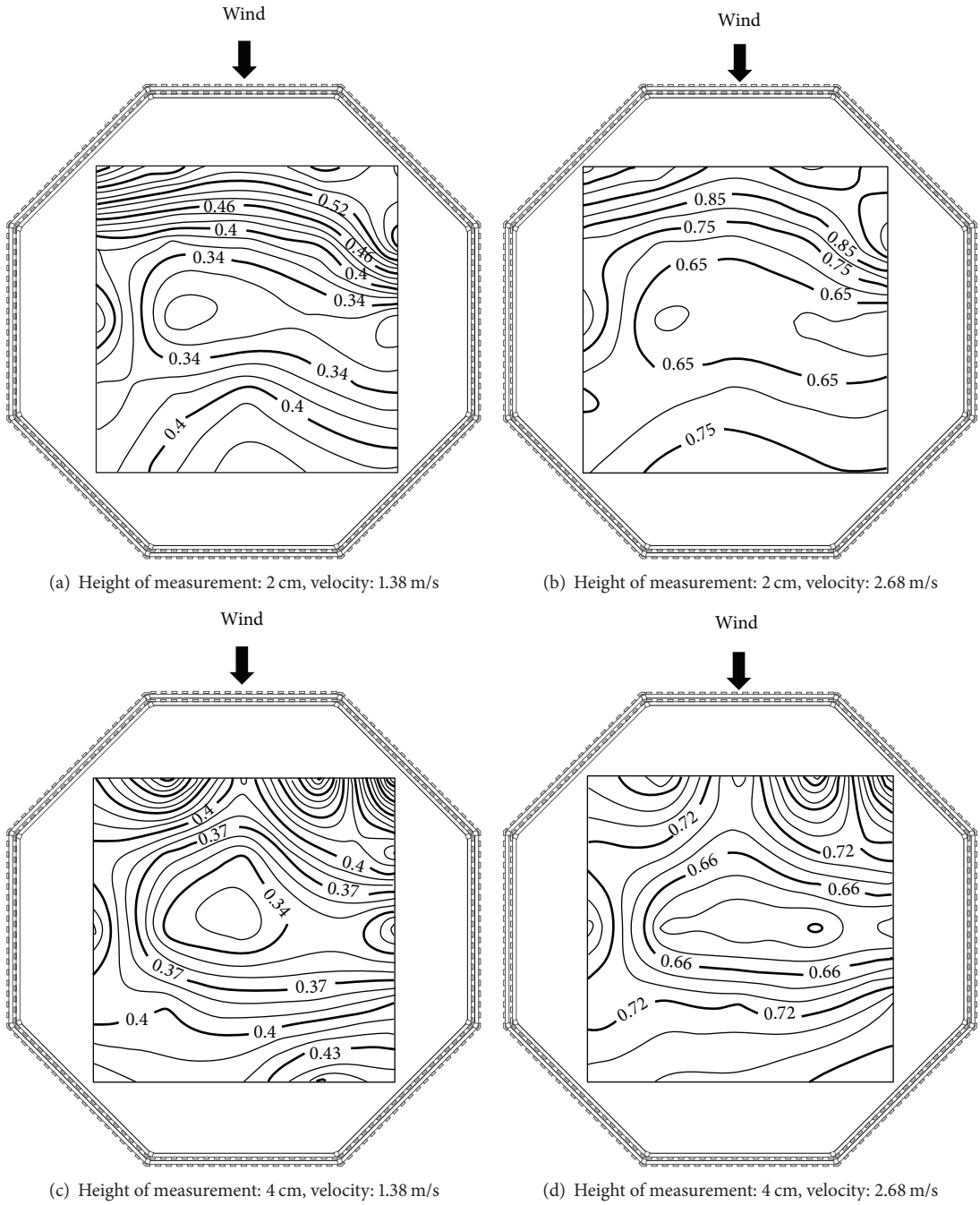

Figure 17: Distribution of wind velocity within the windbreak (CASE 1).

and were verified to have good performance. The period of field measurement was 26 days, from November 4th to November 29, 2012. The anemometers were installed in the Gochang weather station (35°20′N, 126°35′E). Measurement of average and maximum wind velocities was taken over 24 hours, at an interval of one hour. Figure 23 shows average and maximum wind velocities during each time. As the wind velocity was marked more quickly on the anemometers installed outside the models, it is judged that there were wind velocity decrease effects within the windbreaks. The wind velocity decrease rates within the windbreaks varied with the windbreaks' widths. The average wind velocity decreased by 27%–63% inside the windbreak fences, with respect to the velocity outside. The maximal wind velocity decreased by 30%–50% inside the windbreak fences, with respect to the velocity outside. The windbreak fence width of 4 m (model B) turned out to be more effective in decreasing wind velocity rates than the width of 6 m (model A, model C). Using the windbreak width of 6 m, this study has compared the wind velocities within the fences, in the case of the windbreak's

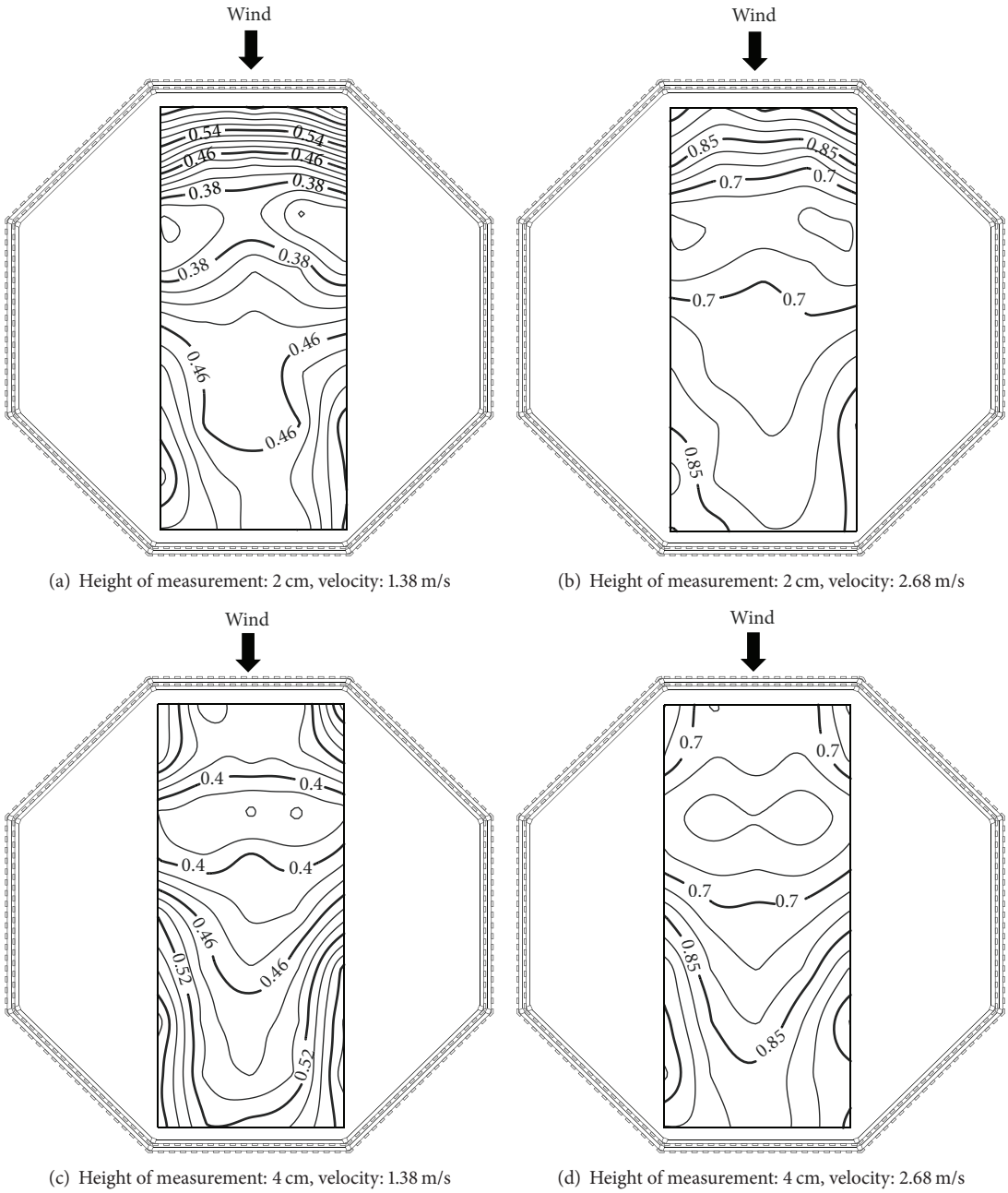

(a) Height of measurement: 2 cm, velocity: 1.38 m/s

(b) Height of measurement: 2 cm, velocity: 2.68 m/s

(c) Height of measurement: 4 cm, velocity: 1.38 m/s

(d) Height of measurement: 4 cm, velocity: 2.68 m/s

Figure 18: Distribution of wind velocity within the windbreak (CASE 2).

fixed vertical bars on the ground and separated from the ground. The maximal velocity was identical in model A, where the windbreak vertical bars were fixed on the ground, and in model C, where they were separated from the ground. However, the average wind velocity turned out to decrease by 10% or more at 9–19 hours in Model A, where the windbreak vertical bars were fixed on the ground, with respect to Model C. The fixed, vertical windbreak bars on the ground were more effective in achieving a significant reduction in wind velocity. Table 3 shows the average and maximum wind velocities measured for 26 days for the field measurement test models. The fence with a 4 m width (model B) showed a 65% decrease in the average wind velocity and a 49% decrease in the maximum wind velocity, when compared with external wind velocity. However, regarding the fence with a 6 m width (models A and B), the average and maximum wind velocity decreased by 47% and 23%, respectively, from the equivalents of external wind velocity.

7. Conclusion

Weather stations plates are set up on the flat ground in meteorological observatories, in order to measure the amount

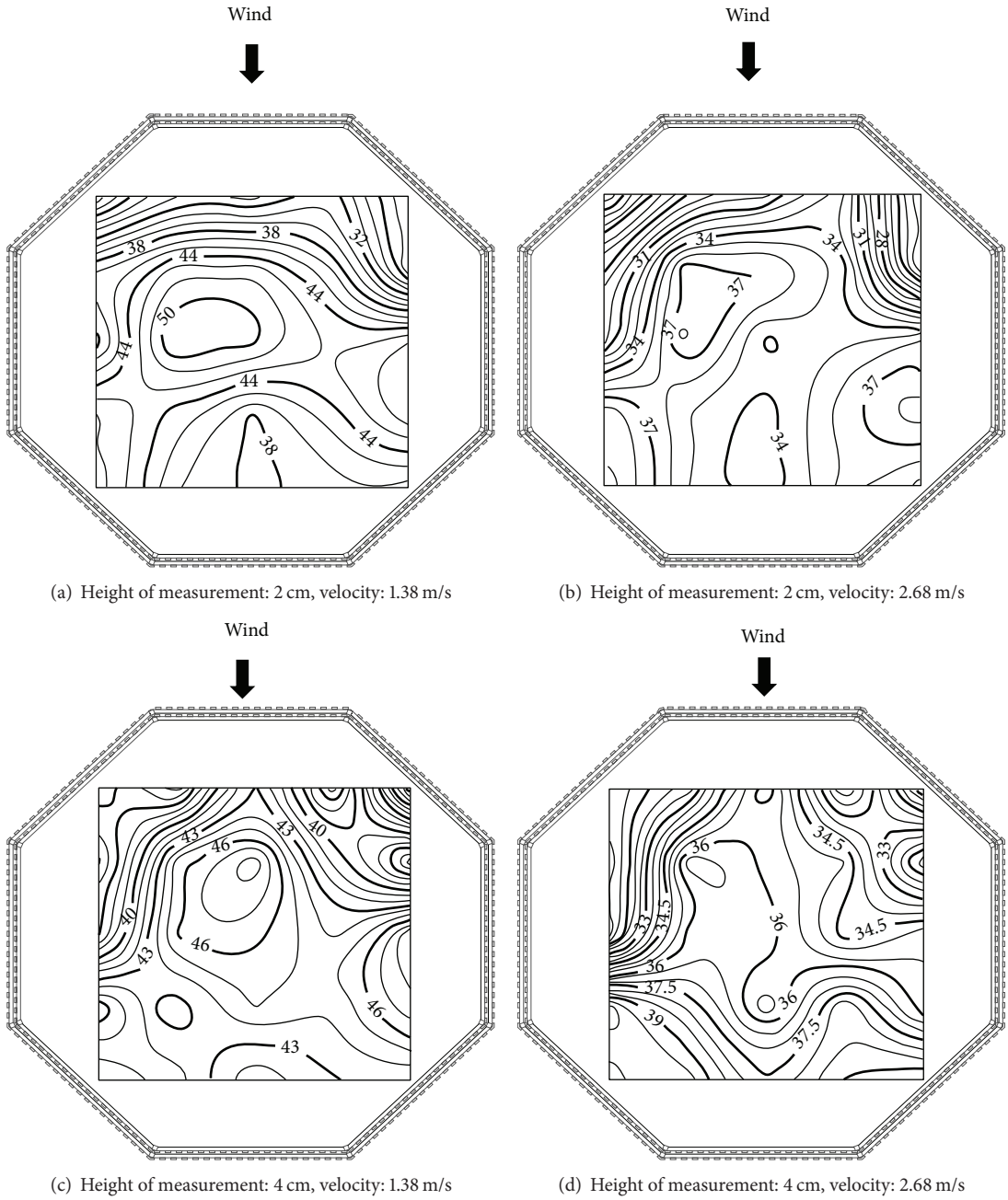

(a) Height of measurement: 2 cm, velocity: 1.38 m/s

(b) Height of measurement: 2 cm, velocity: 2.68 m/s

(c) Height of measurement: 4 cm, velocity: 1.38 m/s

(d) Height of measurement: 4 cm, velocity: 2.68 m/s

Figure 19: Distribution of the turbulence intensity inside the windbreak fence. (CASE 1).

Table 2: Specifications of the windbreaks installed in the weather station (unit = m).

	Width	Height	The distance from the windbreak wings to the ground
Model A	6	0.6	0
Model B	4	0.6	0
Model C	6	0.6	0.15

Table 3: Average and maximum wind velocities by the type of models (unit: m/s).

	Model A	Model B	Model C	Outside
Average	0.40	0.26	0.43	0.75
Maximum	1.49	0.99	1.48	1.93

of snowfall. However, accurately measuring the amount of snowfall covering the ground is hard due to the influence of the wind. The results of the CFD analysis, wind tunnel test, and field measurement (aimed at examining changes in wind velocities within the fences, according to varying fence widths and heights) are as follows.

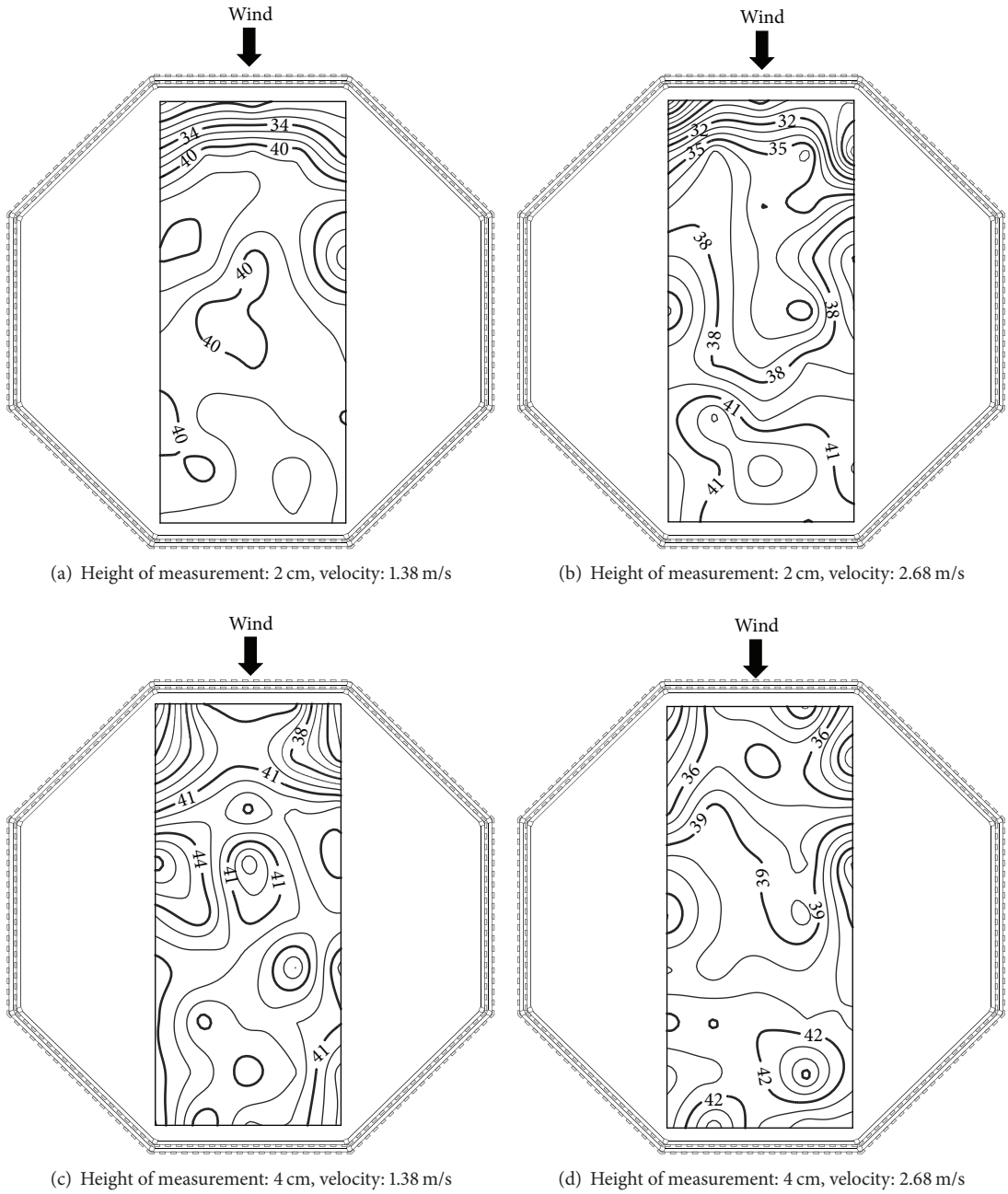

(a) Height of measurement: 2 cm, velocity: 1.38 m/s

(b) Height of measurement: 2 cm, velocity: 2.68 m/s

(c) Height of measurement: 4 cm, velocity: 1.38 m/s

(d) Height of measurement: 4 cm, velocity: 2.68 m/s

Figure 20: Distribution of the turbulence intensity inside the windbreak fence (CASE 2).

According to the result of the CFD analysis of the linear windbreak fences, a double fence whose vertical bars were fixed on the bottom is more effective in decreasing wind velocity. The distance where wind velocity decreased to a maximal extent varied according to the height of fences. The results of the CFD analysis, wind tunnel test, and field measurement of the octagonal windbreak fences showed that the wind velocity decrease rate was greatest at the center of the ooctagonal windbreak, when the fence width was 4 m and its height was 60 cm.

Conflict of Interests

The authors declare that there is no conflict of interests regarding the publication of this paper.

Acknowledgments

This work was supported by the National Research Foundation of Korea (NRF) and was grant funded by the Korea government (MEST) (no. 2011-0028567).

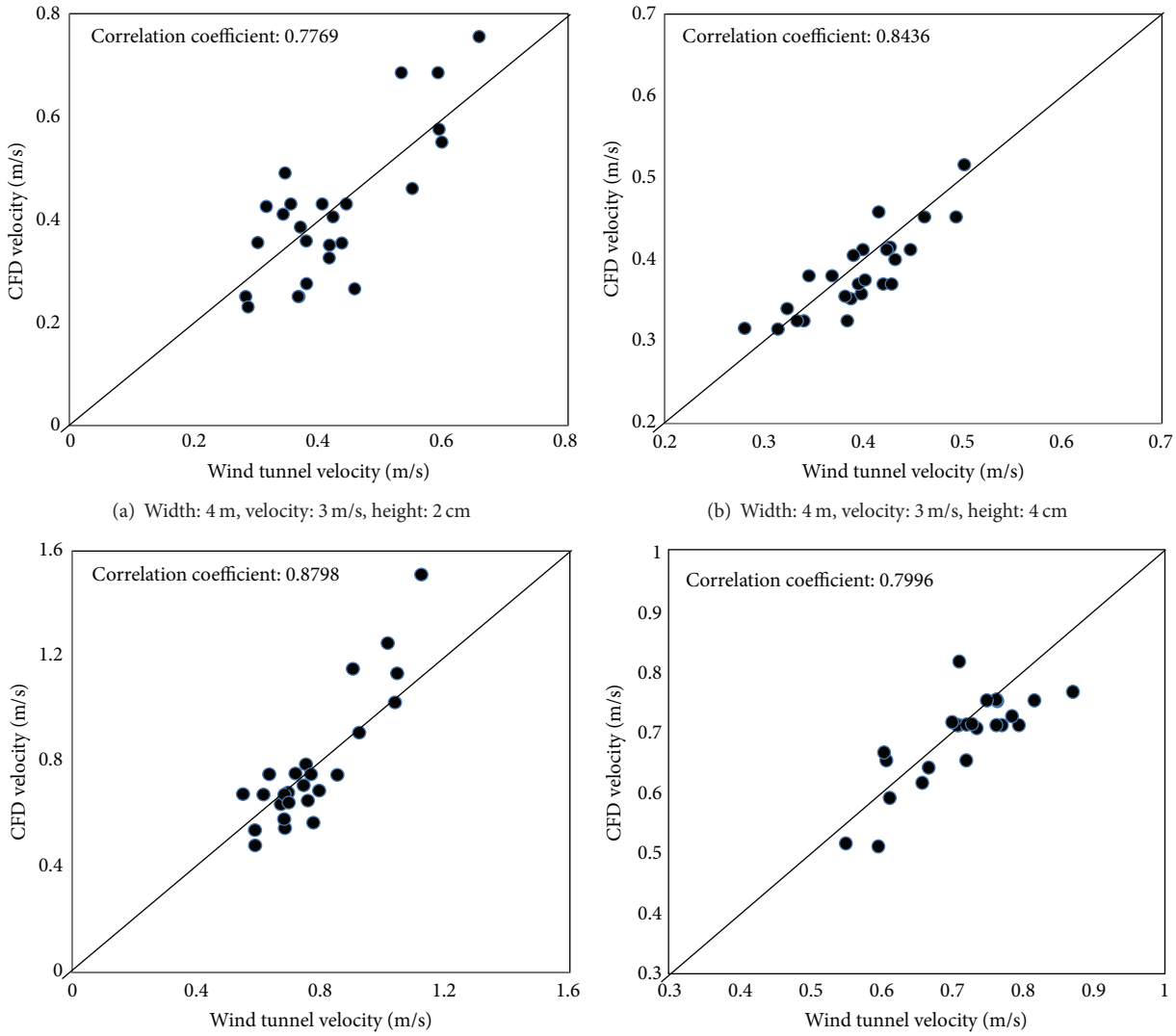

(a) Width: 4 m, velocity: 3 m/s, height: 2 cm

(b) Width: 4 m, velocity: 3 m/s, height: 4 cm

(c) Width: 4 m, velocity: 6 m/s, height: 2 cm

(d) Width: 4 m, velocity: 6 m/s, height: 4 cm

Figure 21: Wind velocity distribution and correlation coefficients for wind tunnel test and CFD.

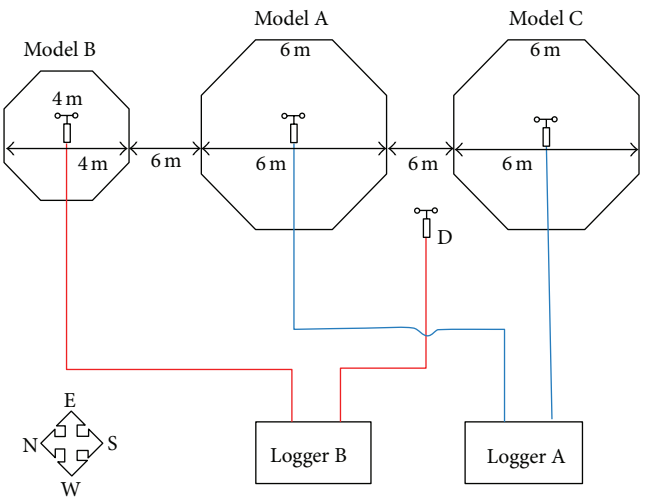

Figure 22: Arrangement plan and measurement process of anemometers.

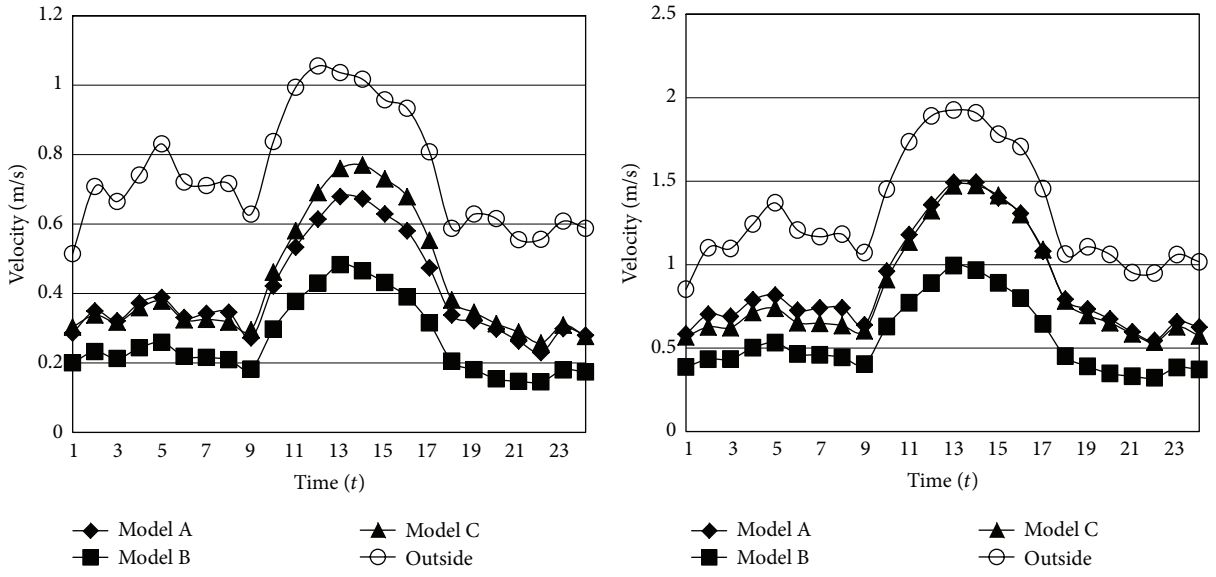

(a) Average wind velocity

(b) 1 hour maximum wind velocity

Figure 23: Average and maximum wind velocities during each time.

References

[1] E. J. Plate, "The aerodynamics of shelter belts," *Agricultural Meteorology*, vol. 8, pp. 203–222, 1971.

[2] M. D. A. E. S. Perera, "Shelter behind two-dimensional solid and porous fences," *Journal of Wind Engineering and Industrial Aerodynamics*, vol. 8, no. 1-2, pp. 93–104, 1981.

[3] K. G. Ranga Raju, R. J. Garde, S. K. Singh, and N. Singh, "Experimental study on characteristics of flow past porous fences," *Journal of Wind Engineering and Industrial Aerodynamics*, vol. 29, no. 1–3, pp. 155–163, 1988.

[4] M. J. Judd, M. R. Raupach, and J. J. Finnigan, "A wind tunnel study of turbulent flow around single and multiple windbreaks, part I. Velocity fields," *Boundary-Layer Meteorology*, vol. 80, no. 1-2, pp. 127–165, 1996.

[5] S.-J. Lee and H.-B. Kim, "Laboratory measurements of velocity and turbulence field behind porous fences," *Journal of Wind Engineering and Industrial Aerodynamics*, vol. 80, no. 3, pp. 311–326, 1999.

[6] C. W. Park and S. J. Lee, "The effects of a bottom gap and non-uniform porosity in a wind fence on the surface pressure of a triangular prism located behind the fence," *Journal of Wind Engineering and Industrial Aerodynamics*, vol. 89, no. 13, pp. 1137–1154, 2001.

[7] scStream Version 9. 0 Cradle co., Japan.

[8] T.-H. Shih, W. W. Liou, A. Shabbir, Z. Yang, and J. Zhu, "A new k-ε eddy viscosity model for high Reynolds number turbulence flow," *Journal of Wind Engineering and Industrial Aerodynamics*, vol. 24, no. 3, pp. 227–238, 1995.

[9] N. G. Wright and G. J. Easom, "Non-linear k-ε turbulence model results for flow over a building at full-scale," *Applied Mathematical Modelling*, vol. 27, no. 12, pp. 1013–1033, 2003.

[10] B. E. Launder and D. B. Spalding, *Lectures in Mathematical Models of Turblence*, Academic Press, London, UK, 1972.

[11] E. Simiu and R. H. Scanlan, *Wind Effects on Structures*, JohnWiley & Sons, 1996.

[12] J. D. Holmes, *Wind Loading on Structures*, Spon, 2001.